Colloids and Surfaces B: Biointerfaces 112 (2013) 294–301

Contents lists available at ScienceDirect

Colloids and Surfaces B: Biointerfaces

journal homepage: www.elsevier.com/locate/colsurfb

Driving forces for the adsorption of a His-tag Chagas antigen. A rational approach to design bio-functional surfaces

Laura E. Valenti[a], Andrea M. Smania[b], Carlos P. De Pauli[a], Carla E. Giacomelli[a,*]

[a] Instituto de Investigaciones en Físico Química de Córdoba (INFIQC) CONICET-UNC, Departamento de Fisicoquímica, Facultad de Ciencias Químicas, Universidad Nacional de Córdoba, Ciudad Universitaria, X5000HUA Córdoba, Argentina
[b] Centro de Investigaciones en Química Biológica de Córdoba (CIQUIBIC) CONICET-UNC, Departamento de Química Biológica, Facultad de Ciencias Químicas, Universidad Nacional de Córdoba, Ciudad Universitaria, X5000HUA Córdoba, Argentina

ARTICLE INFO

Article history:
Received 29 April 2013
Received in revised form 17 July 2013
Accepted 29 July 2013
Available online xxx

Keywords:
H49 antigen
Ni(II) modified substrates
Adsorption mechanism
Bio-affinity interaction
Immunosensor
Direct non-labeled detection

ABSTRACT

In order to rationally design a bio-functional surface based on the adsorption of a His-tag antigen, three requirements have to be considered: the bio-recognition element, the driving forces for the adsorption process and the detection mode of the bio-recognition event. This work is focused on the study of the adsorption mechanism of the His-tag H49 Chagas antigen on Ni(II) modified substrates. In order to construct the bio-functional surface, the gen of the H49 Chagas antigen was modified to incorporate His_6 moiety at the N-terminal (His_6-H49). Then, its physical adsorption and bio-affinity interaction with the solid substrate was studied by reflectometry. Besides His-Ni(II) bio-affinity interactions, His_6-H49 was also physically adsorbed on Ni(II) modified substrates, leading to randomly oriented antigens. These loosely attached bio-molecules were partially removed using conditions of electrostatic repulsion. On the other hand, bio-affinity interactions, resulting in site-oriented molecules on the substrate, were only removable by specific competitors for Ni(II) surface sites. Finally, the surface bio-activity was determined from the peak separations of voltammetry waves due to the change of the electron transfer kinetics of a redox probe through the bio-functional surface (working electrode).

1. Introduction

Chagas is an endemic disease in Latin America (caused by the bite of a bug infected with the protozoan parasite *Trypanosoma cruzi*), affecting around 10 million people, mostly from the low-income side of the society. It is also a concern in other areas because non-checked blood transfusion and solid organ transplantation have become important modes of transmission [1]. There are only a few commercially available kits to detect anti-*T. cruzi* antibodies in serum samples. Most of them are rather unspecific and uncertain [2–4] because they use the total parasite homogenate or a set of antigens from the parasite extract as bio-recognition elements [5–8]. Only recently, the analytical response of indirect labeled immunosensors has been improved by using single recombinant antigens as bio-recognition elements [9].

In order to design a bio-functional surface to be used as a reliable antigen based immunosensor, three requirements have to be considered: (a) a specific antigen to act as bio-recognition element; (b) optimized adsorption conditions (strong antigen–substrate interaction, proper orientation on the substrate, minimized conformational changes of the adsorbed antigen); and (c) a simple, fast and accurate detection method of the bio-recognition event (immune complex formation). The first requirement can be reached with DNA recombinant techniques by engineering immunodominant sequences to express antigens for a particular antibody. On this regard, different structures have been designed and expressed as potential Chagas antigens (CRA, RP1, RP2, and H49 among others) [10,11]. Particularly, H49 is an immunodominant *T. cruzi* antigen consisting of 4.5 tandemly arranged repeated sequences of 68 amino acids [12,13]. These repeat units are largely conserved between strains and isolates of *T. cruzi*, which confer high performance in terms of both specificity and sensitivity for reliable sero-diagnostic tests of Chagas disease [9].

The second requirement represents a rational approach, which is based on the study of the adsorption–desorption process of the antigen, to develop specific, reproducible, and reusable bio-functional surfaces. Solid substrates are usually bio-functionalized by covalent linkage, bio-affinity interactions, or physical adsorption. The first two strategies require the modification of the

* Corresponding author at: Instituto de Investigaciones en Físico Química de Córdoba (INFIQC) CONICET-UNC, Departamento de Fisicoquímica, Facultad de Ciencias Químicas, Universidad Nacional de Córdoba, Pabellón Argentina, Ciudad Universitaria, X5000HUA Córdoba, Argentina. Tel.: +54 3514334169; fax: +54 3514334188.
E-mail addresses: giacomel@fcq.unc.edu.ar, carlaeg@gmail.com (C.E. Giacomelli).

0927-7765/$ – see front matter © 2013 Elsevier B.V. All rights reserved.
http://dx.doi.org/10.1016/j.colsurfb.2013.07.059

substrate and/or the antigen, which may lead to conformational changes of the bio-molecule. However, these strategies induce strong and stable interactions between the antigen and the substrate [14]. On the other hand, physical adsorption does not require modifications while comprising many drawbacks, like weak attachment, random orientation and conformational perturbation, reducing the surface biological activity. Bio-affinity reactions offer a gentle site oriented bio-functionalization procedure, providing important advantages over other strategies [15,16]. Among others, the interaction between His-tag (usually His_6) proteins and surface metal cations (Ni^{2+}, Cu^{2+}, Co^{2+} or Zn^{2+}), generates high affinity surface chelate complex [17,18]. His-tag can be genetically introduced into recombinant proteins at the N- or C-terminal as well as in exposed loops of the protein. Furthermore, the fact that many commercially available protein expression plasmid vectors include His-tag (to facilitate the purification step [19]), makes this bio-functionalization procedure widely used.

Finally, immunosensors are mostly coupled to indirect methods to detect the immune complex formation which, are usually highly sensitive to the antibody presence in the sample [20,21]. However, these methods are time-consuming (involving bio-molecules labeling and complex solution handling) and present problems due to nonspecific binding effects. On the other hand, direct detection methods rely on a measurable signal (potential difference, current, resistance, mass, heat, or optical properties) caused by the bio-recognition event [22,23]. Immunosensors coupled to direct detection methods are capable of real-time monitoring of a wide range of molecules with low detection limits. Particularly, electrochemical immunosensors offer some advantages, such as high sensitivity, rapid, inexpensive and easy adjustment to micro or nano fabrication [24].

This work discusses a rational approach to design a reliable biofunctional surface assembled with the His-tag H49 Chagas antigen [25] and Ni(II) modified substrates [26]. The first part of the discussion is concerned with the expression and purification of the recombinant H49 that was engineering with a His_6-tag at the N-terminal (His_6-H49). The incorporation of the His_6-tag in the H49 primary structure (by the modification of the gene that encodes for this antigen) facilitates the purification step, as well as induces the bio-affinity interaction with Ni(II) surface sites trough its N-terminal [17]. The second part of the discussion, refers to the bio-affinity and physical interactions between His_6-H49 and Ni(II) modified substrates, with a special emphasis on the adsorption mechanisms and desorption behavior upon addition of different agents. Finally, the surface bio-activity was evaluated with a direct, label-free electrochemical method using sera samples. This piece of evidence is crucial because it represents the first step toward optimizing a stable and specific Chagas immunosensor coupled to a direct non-labeled detection method.

2. Experimental

2.1. Materials

2.1.1. Bacterial strains, plasmids, and reagents

Escherichia coli BL21, and the expression vector pET-15b were obtained from Novagen; pGEM-T Easy plasmid for cloning PCR products, isopropyl-β-D-thiogalactoside (IPTG), and the restriction enzymes *NdeI* and *BamHI* from Promega; His-bind resin "Probond", and Pfx DNA polymerase from Invitrogen; bovine serum albumin (BSA), and 3-aminopropyltrimethoxysilane (APTMS) from Sigma; cysteamine (Cyst), and $NaBH_4$ from Fluka; absolute ethanol, acetic anhydride (Ac_2O), pyridine, histidine (His), and imidazole (Imi) from Anhedra; and glutaraldehyde (Glut), $Ni(NO_3)_2{\cdot}6H_2O$, $NaH_2PO_4{\cdot}7H_2O$, and NaCl from Baker. All reagents were of analytical grade and used without further purification.

pGEXA plasmid encoding the H49 immunodominant recombinant antigen was kindly provided by J. F. Da Silveira (UNIFESP, Sao Paulo, Brazil) [13]; blinded serum samples from chronic chagasic (positive sera) and non-chagasic (negative sera) patients, and total *T. cruzi* homogenate by S. Gea (CIBICI-UNC, Córdoba, Argentina) and E. Moretti (Instituto Nacional de Chagas, Córdoba, Argentina), respectively.

Aqueous solutions were prepared in deionized water (Milli Q System, Millipore). The pH measurements were performed with a glass electrode and a digital pH meter (Orion 420 A+, Thermo). All experiments were performed at room temperature ($26 \pm 2\,^{\circ}C$) unless otherwise stated.

2.1.2. Substrates

The substrate modification to expose Ni(II) surface sites was conducted on silica or gold depending on the experimental determination (i.e. silica was used to study the adsorption–desorption mechanism by reflectometry while gold was employed to determine the surface bio-activity electrochemically). The polycrystalline gold substrates (99.99% purity) were 0.3 mm-thick plates with dimensions of 0.5 cm × 1.5 cm, while 100 nm-thick layers of silica were prepared by oxidizing silicon wafers (100 mm, Silicon Valley Microelectronics Inc., Santa Clara, CA, USA) at 1000 °C for 1 h [27]. Before use, both substrates were immersed in a boiling piranha solution (H_2SO_4:H_2O_2; 3:1) for 30 min, rinsed thoroughly with deionized water and dried under an N_2 flow. (*Caution! Piranha solution is a powerful oxidizing agent that reacts violently with organic compounds; it should be handled with extreme care*). In addition, gold substrates were cycled in 0.5 mol L^{-1} H_2SO_4 50 times (between 0.00 and 1.55 V vs. Ag/AgCl/KCl_{sat}). On the other hand, silica substrates were further treated with air plasma (Harrick Plasma) for 20 min. The substrates were used immediately after completion of the cleaning procedure.

3. Methods

3.1. Substrates modification

Ni(II) modified substrates (either gold or silica) were prepared in multiple steps [26] which began with the formation of an amino-terminated SAM: gold incubated in Cyst and silica in APTMS. In the second step, the amino-modified substrates were incubated in Glut, which was followed by incubation in Ac_2O and the reaction with aqueous $NaBH_4$. Finally, the substrates were stored in aqueous Ni(II) solution until further use. With gold and silica substrates, the modified substrate exposed carboxylate groups that partially coordinate Ni(II) ions [26] providing an appropriate environment for the bio-affinity interaction. Imidazole groups of the His-tag easily removed water molecules from the Ni(II) coordination sphere [28].

3.2. His_6-H49 recombinant antigen expression and purification

A 1 kb DNA fragment containing the coding region of the H49 gene was amplified by PCR from the plasmid pGEXA using the oligonucleotides 5′-CATATGCCCCGGTCAGAATTCCTGGC-3′ and 5′-GGATCCTCAAAGCTTCAGATCTCTGAATTC-3′ as forward and reverse primers, respectively (underlined regions indicate *NdeI* and *BamHI* restriction sites). PCR assays were conducted under the following conditions: 1 min at 95 °C, 30 cycles of 20 s at 94 °C, 1 min at 68 °C and 1 min at 72 °C, and a final extension of 5 min at 72 °C. The PCR product was extracted from agarose gels with a gel purification kit (Qiagen) and cloned into the pGEM-T Easy vector (Promega). After the digestion with *NdeI* and *BamHI* restriction enzymes, H49 was inserted into the respective sites of the pET-15b expression vector

to generate pET-H49 plasmid, which encoded the H49 recombinant antigen fused in frame to an N-terminal His_6 tag (His_6-H49).

His_6-H49 antigen was over-expressed in *E. coli* BL21. A single colony of transformed *E. coli* harboring the pET-H49 plasmid were inoculated into 3 mL of LB media (1.0% NaCl, 1.0% soy peptone and 0.5% yeast extract) containing 200 μg/mL ampicillin (Amp) and 0.5% glucose and grown overnight at 37 °C with shaking at 220 rpm. Overnight culture was inoculated into 1 L of the same media, grown to OD_{600} of 0.6 at 37 °C with shaking at 220 rpm. The expression of His_6-H49 was induced by addition of 1 mmol L^{-1} IPTG. After 1 h of induction, cells were harvested by centrifugation, resuspended in buffer A (15% glycerol, 0.5 mol L^{-1} NaCl, 20 mmol L^{-1} Tris–HCl, pH 7.5), and lysed by lysozyme treatment (0.5 mg mL^{-1} on ice for 30 min) followed by 5 cycles of freezing/thawing and pulsed ultrasonication. The lysate was centrifuged at 10.000 rpm at 4 °C for 30 min and the supernatant was incubated with the His-bind resin (1 mL resin/1 L supernatant) during 3 h at 4 °C with shaking after which it was loaded onto a column. After washing with 6 column volumes of buffer A, the recombinant protein was eluted by successive washes with buffer A supplemented with 60, 80 and 400 mmol L^{-1} Imi. The eluted fractions were further loaded onto a Sephadex G25 column and washed with 5 mmol L^{-1} phosphate buffer pH 7.0 to remove Imi. His_6-H49 was lyophilized for 48 h, stored at −70 °C and analyzed on sodium dodecyl sulfate-polyacrylamide gel electrophoresis (SDS-PAGE). Protein was obtained with a purity >95%.

The bio-activity of His_6-H49 antigen was detected by Western blot using positive and negative chagasic sera. Following SDS-PAGE (12% polyacrylamide), in 90 mM Tris/borate, 1 mM EDTA (TBE) and 0.1% SDS, proteins were transferred to a nitrocellulose membrane by electroblotting (20%, v/v; methanol, 0.1% SDS using TBE as running buffer at 400 mA during 45 min). The nitrocellulose was blocked with 5% skim milk in TTBS (50 mmol L^{-1} Tris pH 8, 200 mmol L^{-1} NaCl, 0.05% Triton X-100) for 1 h with gentle rocking. The membrane was washed with TTBS and incubated with 1/100 dilution of sera at room temperature for 1 h. After washing with TTBS, the membrane was incubated with a horseradish peroxidase labeled anti-mouse IgG which was then detected by peroxidase activity on 4-chloro-1-naphtol used as chromogenic substrate.

3.3. His_6-H49 adsorption–desorption

The adsorption–desorption process was followed by reflectometry as described elsewhere [27] using modified silica in the absence (silica/COO) and presence of Ni(II) (silica/COO-Ni(II)). Briefly, from 0 to 200 s, only buffer was introduced into the cell and a stable baseline was obtained. Then (from 200 to 1200 s), the flow was switched from buffer to a His_6-H49 solution (prepared in the same buffer). Next (between 1200 and 1600 s), the flow was switched back to the initial buffer solution in order to analyze the desorption process by dilution. The experiments were conducted with His_6-H49 antigen at different concentrations (ranging from 0.1 to 10.0 μg/mL) in PB (5 mmol L^{-1} phosphate buffer pH 8.0) and non-tagged commercial BSA (10.0 μg/mL) in PB and PB + NaCl (5 mmol L^{-1} phosphate buffer pH 8.0 + 100 mol L^{-1} NaCl). The desorption process was evaluated by dilution with PB, followed by the addition of surfactants (4.0 mmol L^{-1} SDS, 0.5 mmol L^{-1} CTAB or 0.1%, v/v, Tween 20), 0.2 mol L^{-1} NaCl, 0.2 mol L^{-1} His, or 0.5 mol L^{-1} Imi solutions prepared in PB. Control experiments were also performed by reflectometry to evaluate the adsorption of surfactants on the modified substrates without an adsorbed protein layer.

It is important to note that changes in the ionic strength, due to the presence of ionic species in the desorption solutions, prevented a direct assessment of the desorbed amount by reflectometry. Thus, the desorbed amount was determined indirectly in the following way: (a) previously adsorbed His_6-H49 antigens (10.0 μg/mL in PB) were rinsed with PB, re-adsorbed and rinsed again to check the reversibility of the adsorption–desorption process; (b) the reflectometer measurement was paused and the cell was filled with the corresponding desorption solution (His, Imi or NaCl) for 20 min; (c) the cell was rinsed with PB to measure the protein re-adsorbed amount of a new incoming His_6-H49 antigen (10.0 μg/mL in PB) solution. Desorption percentages were calculated from the saturation adsorbed amounts measured in steps (a) (100%) and (c), assuming that the new incoming His_6-H49 antigen in this step occupied the uncovered surface caused by desorption induced in step (b). This assumption was valid because the adsorption–desorption cycles in (a) were fully reversible.

As described elsewhere [27], to calculate the sensitivity factor (Q-factor) that provides the proportionality constant between the measured signal and the adsorbed amount, the substrate was modeled as a silicon substrate (refraction index of 3.80) with a 100 nm silica layer (refraction index of 1.46) immersed in aqueous solution (refraction index of 1.333) and the increment in the refraction index with the protein concentration (dn/dc) was considered to be 0.18 [29]. The calculated Q-factors resulted in 27 mg m^{-2} for BSA and 24 mg m^{-2} for His_6-H49.

Recalling that the protein transport toward the substrate was well controlled by the stagnation point flow of the reflectometer setup, the supply rate depended on the geometry of the cell, the flow rate, the diffusion coefficient of the macromolecule (D), and its concentration in solution (C_p) [30–32]. Hence, for a particular cell setup and protein molecules, the supply rate was directly proportional to C_p. The proportionality coefficient provided the transport constant ($k = 4 \times 10^{-6}$ m s^{-1}) of the protein ($D = 6 \times 10^{-11}$ m^2 s^{-1}) at the specified cell setup.

3.4. His_6-H49 surface bio-activity

The surface biological activity was evaluated by cyclic voltammetry (CV) using Ni(II) modified gold substrates (gold/COO-Ni(II)) and a redox probe composed by 0.5 mmol L^{-1} $K_3Fe(CN)_6$ and 0.5 mmol L^{-1} $K_4Fe(CN)_6$ (50 mmol L^{-1} PB). To this end, the working electrode was the bio-functional surface prepared by dipping the gold/COO-Ni(II) substrate in 10.0 μg/mL His_6-H49 (in PB) for 30 min, by rinsing to remove physically adsorbed antigens, and by blocking free surface sites with 0.25% w/v BSA prepared in TPBS (PB pH 8.0 + 0.2 mol L^{-1} NaCl + 0.1% v/v Tween 20 for 60 min). The experiments were performed in an electrochemical analyzer coupled to a personal computer (Chi instruments) and carried out in a three electrode conventional cell, including a $Ag/AgCl/KCl_{sat}$ reference electrode, and a Pt counter electrode. The electrochemical behavior of the redox probe was analyzed before and after the immunoreactions over the −0.2 to 0.5 V range at different scan rate (20–300 mV s^{-1}) using 50 mmol L^{-1} PB as supporting electrolyte. The immunoreaction was carried out with positive and negative (as control) sera (dilution 1/100 in TPBS) for 60 min, followed by TPBS rinsing prior to the electrochemical measurements. These measurements were performed on independent substrates by triplicate experiments at room temperature. To determine the performance of the bio-functional surface, the electrochemical response to negative and positive sera were compared by two-way statistic ANOVA analysis with 95% confidence. Scan rate and serum nature were the two treatments used to determine significant differences ($p < 0.05$) between positive and negative samples.

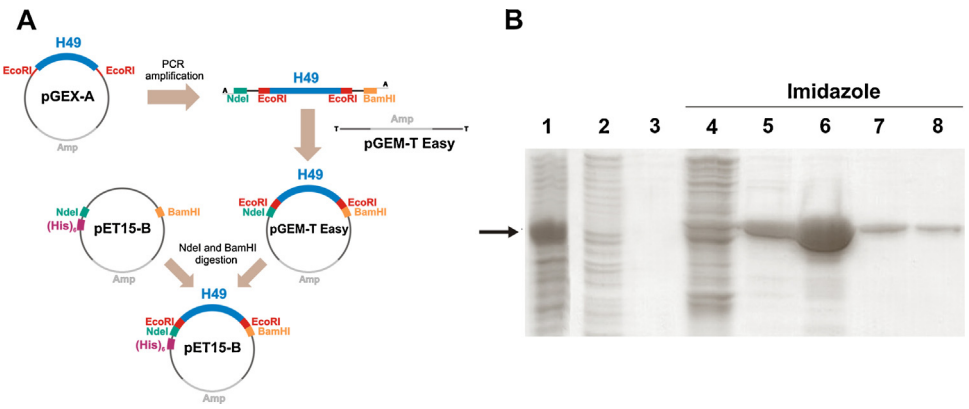

Fig. 1. (A) Cloning strategy employed to incorporate the His_6 moiety at the H49 N-terminal. A 1000 bp fragment containing the coding region of H49 antigen was amplified by PCR from the pGexA plasmid, ligated to the pGem-T Easy vector and subsequently cloned into the plasmid pET-15B by using the 5′ *NdeI* restriction site, which allowed an in frame fusion to a six His tag at the N-terminal of H49 antigen. (B) Analysis of an SDS/polyacrylamide gel stained with Coomassie Brilliant Blue that was loaded with the 100.000 × *g* supernatant of extracts from pET-*His_6H49*-transformed BL21 *E. coli* cells after IPTG induction (lane 1). Purification protein steps after His-bind resin show proteins that were eluted from de column (lane 2), proteins eluted by washing with buffer A (lane 3) and those eluted by 60 mM (lane 4), 80 mM (lane 5) and 400 mM Imi (lanes 6–8). The arrow indicates the position of the 40 kDa His_6-H49 recombinant antigen.

4. Results and discussion

4.1. His_6-H49 recombinant antigen

Fig. 1A shows the strategy employed to modify the H49 gen in order to incorporate the His_6 moiety at the N-terminal antigen region (i.e. the plasmid leading to the expression of His_6-H49 antigen). Fig. 1B includes the SDS-PAGE performed during the consecutive purification steps demonstrating that the His_6 moiety was successfully incorporated to the H49 primary structure to generate the recombinant His_6-H49 antigen (40 kDa). Moreover, SDS-PAGE analysis indicated that only high concentrations of Imi solutions were able to remove the antigen from the His-bind resin. It is important to note that, although it was established some years ago that H49 was an immunodominant *T. cruzi* antigen [12,13], this is the first report describing the incorporation of the His-tag to the antigen. As depicted in Fig. 2, the bio-activity of recombinant His_6-H49 was checked by Western blot assays using sera from chagasic and non-chagasic patients as antibody sources. The negative sera presented no reaction neither with the antigens in total *T. cruzi* homogenate nor with His_6-H49 (Fig. 2C). On the contrary, an intense reaction was revealed between both, the total homogenate and His_6-H49, when positive Chagas sera were tested (Fig. 2B). Therefore, the designed His_6-H49 recombinant antigen is specifically and sharply recognized by antibodies in positive Chagas sera, which demonstrates its potential to be used in immunosensor devices. Moreover, these bio-activity assays indicate that specificity and sensitivity of His_6-H49 are comparable to those of the antigen without the tag [12].

On the other hand, the isoelectric point (IEp) of the expressed antigen based on the acid dissociation constants of the N- and C-terminal and the side chains of the amino acids (calculated with the Protein Sequence Analysis software) was found to be 5.3. Finally, the hydrophobic/hydrophilic profile of His_6-H49 (calculated on the ExPASy Server [33]) indicated that five highly hydrophilic sites (related to the primary structure repetition) represented the potentially antigenic sites.

4.2. His_6-H49 adsorption–desorption

The adsorption of the His_6-H49 antigen was induced at pH 8.0 to promote the bio-affinity interaction while minimizing physical adsorption. It was previously demonstrated that the complex formation between His_6 and Ni(II) in aqueous solution only occurred at pH > 4 [17]. Further, it was established that adsorbed His_6 on bare silica substrates was easily removed by buffer dilution at pH 8 [34]. Finally, electrostatic interactions between the antigen (IEp 5.3) and the negatively charged substrate [26] were also minimized at this pH, while keeping the biological activity of His_6-H49 (Fig. 2). However, physical adsorption could not be completely removed even under these unfavorable conditions. Table 1 compares the initial adsorption rate (r_{ia}) and the saturation adsorbed amount (Γ_{sat}) of two proteins physically adsorbed (BSA and His_6-H49) and the His-tag antigen when inducing the bio-affinity interaction with

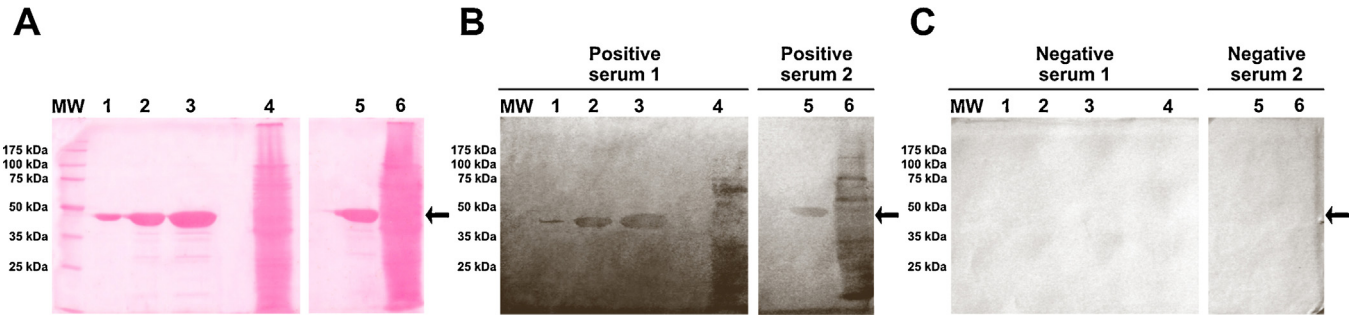

Fig. 2. Different quantities of purified His_6-H49 recombinant antigen (lane 1: 1 mg; lanes 2 and 5: 5 mg; lane 3: 10 mg) as well as total *T. cruzi* homogenate (lanes 4 and 6) were electrophoresed by 12% SDS-PAGE and electrotransferred following Ponceau Red staining (A). Proteins were analyzed by Western blot using positive (B) or negative (C) chagasic sera. Arrows indicate the position of the 40 kDa His_6-H49 recombinant antigen. MW, Molecular Weight Marker (Broad range protein molecular mark, Promega).

Table 1
Initial adsorption rate ($r_{ia} \times 10^{-3}$ in mg m^{-2} s^{-1}) and saturation adsorbed amount (Γ_{sat} in mg m^{-2}) of 10.0 μg/mL BSA and His$_6$-H49 at pH 8.0 on modified silica substrates in the absence (silica/COO) and presence of Ni(II) (silica/COO-Ni(II)).

	Non-tagged protein				His$_6$-H49	
	PB + 100 mM NaCl		PB		PB	
	r_{ia}	Γ_{sat}	r_{ia}	Γ_{sat}	r_{ia}	Γ_{sat}
Silica/COO	10	0.5	2	0.2	8	0.2
Silica/COO-Ni(II)	8	0.8	6	0.3	17	0.5

Ni(II) surface sites. Physical adsorption was evaluated with (a) a model non-tagged protein (10 μg/mL BSA) on silica/COO and silica/COO/Ni(II) at low (PB) and high (PB + 100 mmol L^{-1} NaCl) ionic strength and (b) His$_6$-H49 on silica/COO in PB. BSA was selected as the model non-tagged protein because its molecular weight (60 kDa) and IEp (4.8) roughly coincide with those of the His-tag antigen. In any given condition, r_{ia} values were lower than the supply rate (41×10^{-3} mg m^{-2} s^{-1}) due to the electrostatic barrier for the first protein-substrate contact. Both r_{ia} and Γ_{sat} values were dependent on the ionic strength and the Ni(II) presence indicating that the whole process (from the first protein attachment up to the final conformation of adsorbed molecules) was ruled by electrostatic interactions. At low ionic strength, Γ_{sat} of His$_6$-H49 on silica/COO was of the same magnitude as the non-tagged protein on both substrates, suggesting that these adsorption layers were built in more or less the same fashion. On the other hand, Γ_{sat} for His$_6$-H49 on Ni(II) modified substrate was higher than the value measured with the non-tagged protein pointing to different adsorption features. Therefore, electrostatic interactions dictated the initial antigen–substrate contact while protein–protein repulsion, determining Γ_{sat} with physically adsorbed proteins, were overcome when bio-affinity interactions were feasible.

Fig. 3A shows the adsorption kinetics profile of His$_6$-H49 on silica/COO substrate at different protein concentrations whereas Fig. 3B displays the kinetics curves normalized by the supply rate ($t \times C_p$). Despite the magnitude of the error bars, these curves did not merge indicating that Γ_{sat} values were not exclusively determined by the protein concentration in solution [35]. In other words, the antigen surface coverage was controlled by kinetics rather than thermodynamics reasons [35,36], which is representative of two competitive processes. After the first protein attachment, the molecules optimize their interaction with the substrate, leading to relaxation with some degree of spreading [37]. The extent of this step depends on the ratio between the optimization rate and the filling rate. When the optimization rate is much faster than the filling rate, all the proteins have the same conformation in the final state and the saturation adsorbed amounts do not depend on the supply rate. On the other side, when the optimization process is much slower than the filling rate, the saturation adsorbed amounts are also independent of the supply rate because the substrate crowding is so fast that prevents protein–substrate optimization. Finally, when the characteristic times of both processes are of the same order, the saturation adsorbed amounts are affected by the supply rate because the optimization step strongly depends on the surface coverage (i.e. Γ_{sat}).

Fig. 4A shows the characteristic filling time (τ_{75}) as a function of Γ_{sat} for His$_6$-H49 adsorbed on silica/COO substrate in the absence (triangles) and presence (squares) of Ni(II). This particular definition of the filling time (τ_{75}: the time needed to reach 75% of Γ_{sat}) reported by Wertz and Santore [35], does not assume transport controlled kinetics and it is relatively insensitive to the detailed shapes of the individual adsorption kinetic curves. Considering that protein molecules continuously attach and optimize their interaction

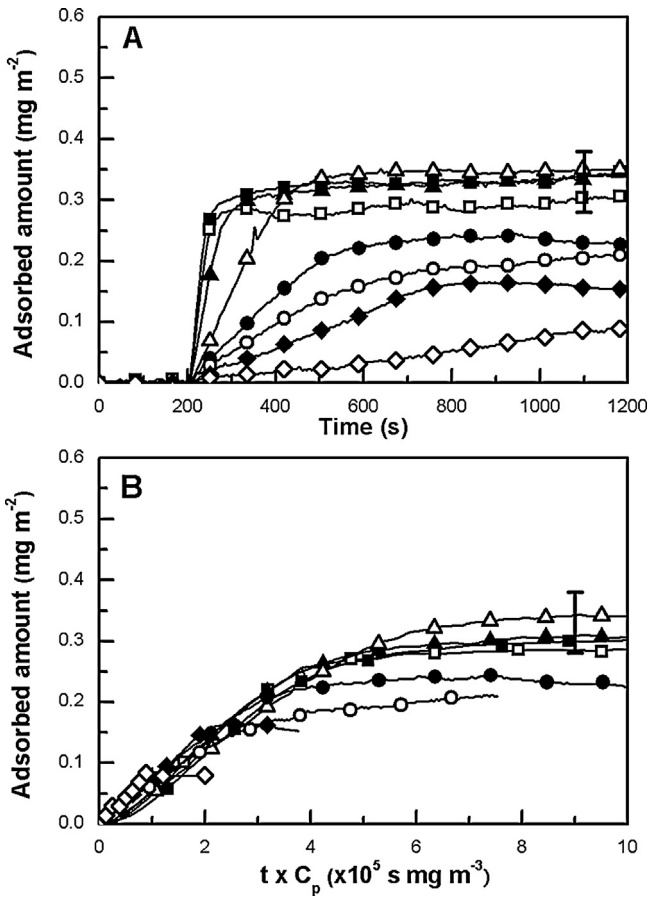

Fig. 3. Adsorption kinetics profiles (A) and kinetics curves normalized by the supply rate (B) of His$_6$-H49 on silica/COO substrate in PB at different concentrations: 10.0 μg/mL (■), 7.5 μg/mL (□), 5.0 μg/mL (▲), 2.5 μg/mL (△), 1.0 μg/mL (●), 0.8 μg/mL (○), 0.4 μg/mL (♦) y 0.1 μg/mL (◊). The error bars indicate the standard deviation of three repeats.

reaching an average surface area per molecule, this parameter allows estimating an average filling rate. The characteristic optimization time (τ_{op}) was estimated by extrapolating to zero Γ_{sat}; in such a condition, a protein molecule has enough room to optimize its interaction without any neighboring molecule hampering the process. Fig. 4B displays the percentage of desorbed proteins from silica/COO substrate in the absence (triangles) and presence (squares) of Ni(II) upon rinsing with PB solution as a function of Γ_{sat}. For physically adsorbed His$_6$-H49, τ_{75} and τ_{op} (~900 s) were of the same order, particularly at low surface coverage ($\tau_{75} \sim 700$ s). As expected from the results of Fig. 3B, these two processes took place at the same time scale (i.e. they are competitive). Furthermore, τ_{75} and the percentage of desorbed molecules linearly diminished as the surface coverage increased.

The time scale corresponding to the filling and desorbing processes are rather different: the first one represents the initial protein–substrate interaction while the second one accounts for the strength of the interaction after the optimization stage. At low filling rate, low surface coverage was reached and attached His$_6$-H49 had enough time and room to spread on the substrate, preventing buffer desorption. On the other side of the plot, the filling rate was rather high and, hence, some of the attached molecules did not have time and room to spread. At high degree of surface coverage, protein molecules were spread to different extent so a percentage of them were desorbed by adding buffer. Consequently, physical adsorption was partially removed by rinsing with buffer at high degree of surface coverage.

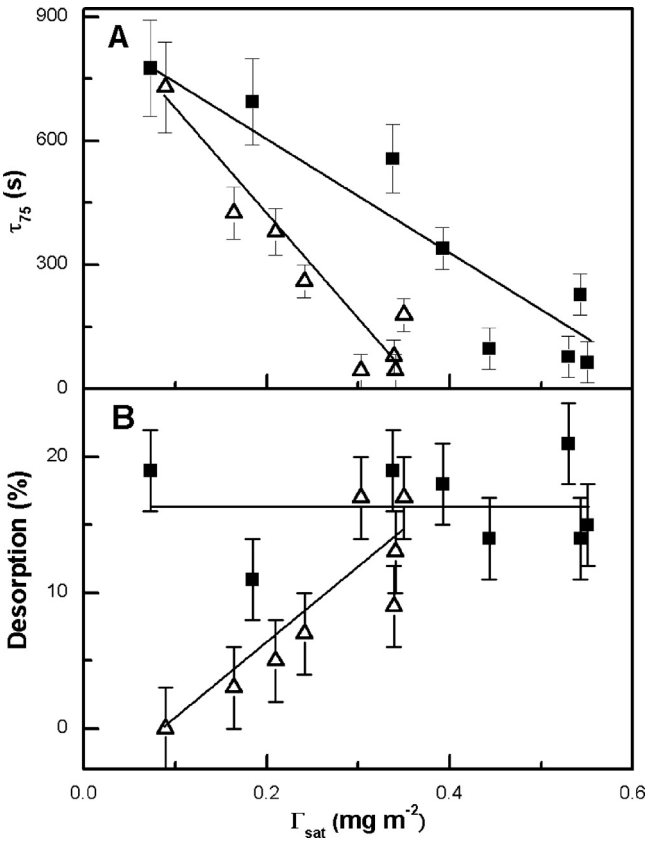

Fig. 4. Characteristic filling time (τ_{75}, A) and desorption percentages upon rinsing with PB (B) as a function of the saturation adsorbed amount (Γ_{sat}) of His_6-H49 on silica/COO (Δ) and silica/COO-Ni(II) (■) substrates. The error bars indicate the standard deviation of three repeats.

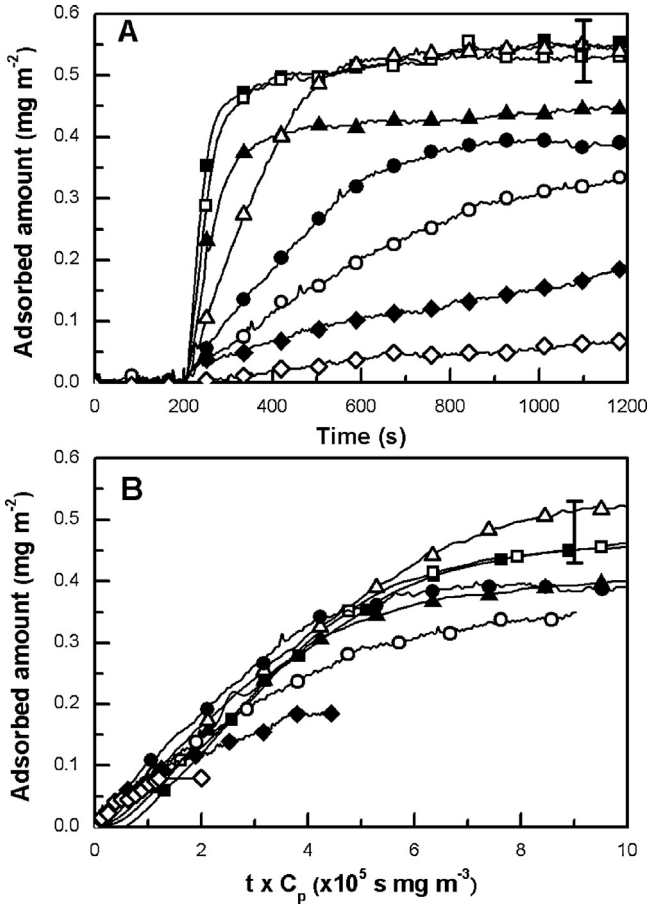

Fig. 5. Adsorption kinetics profiles (A) and kinetics curves normalized by the supply rate (B) of His_6-H49 on silica/COO-Ni(II) substrate in PB at different concentrations: 10.0 μg/mL (■), 7.5 μg/mL (□), 5.0 μg/mL (▲), 2.5 μg/mL (Δ), 1.0 μg/mL (●), 0.8 μg/mL (○), 0.4 μg/mL (♦) y 0.1 μg/mL (◊). The error bars indicate the standard deviation of three repeats.

It is important to note that the desorption behavior of physically adsorbed proteins (His_6-H49 or non-tagged BSA) upon buffer addition was rather different at high degree of surface coverage (data not shown). In contrast to His_6-H49, BSA was not removed from the substrates (either in the absence or presence of Ni(II) sites) indicating that the non-tagged protein was adsorbed on the substrates through more molecule segments. As reported in many works [27,38,39], BSA is a soft protein that easily undergoes conformational changes upon adsorption. On this regard, the conformation of His_6-H49 appeared to be more stable toward surface perturbation.

Fig. 5A and B shows the adsorption kinetics profile and normalized kinetics curves by the supply rate ($t \times C_p$) of His_6-H49 on silica/COO-Ni(II) substrate at different protein concentrations, respectively. The normalized kinetics curves did not merge indicating that also in this case, there were two competitive processes occurring in the same time scale when the His-tag antigen was attached to the Ni(II) modified silica. According to the values of the initial adsorption rate (Table 1), the first contact between His_6-H49 and silica/COO-Ni(II) substrate was electrostatic in nature. Hence, the filling time was calculated as indicated for the physically adsorbed antigen (Fig. 4A, squares). As it was the case with the protein physically adsorbed, τ_{75} and τ_{op} were of the same order and τ_{75} linearly diminished with increasing Γ_{sat}. However, the desorbed percentage (around 15%) was invariant with Γ_{sat} and comparable to the highest amount observed with physically adsorbed proteins (Fig. 4B, triangles), indicating that after the optimization step there were two populations of adsorbed molecules: loosely and strongly attached.

The desorption behavior suggested that spreading of adsorbed molecules could be ruled out as responsible for the competition between the optimization and filling processes (linear behavior between τ_{75} and Γ_{sat}) when His_6-H49 was adsorbed on Ni(II) modified substrates. Based on the low removed amount (15%), the optimization stage comprised a strong antigen attachment that may involve bio-affinity interaction between His residues and Ni(II) surface sites. In such a situation, the competitive processes may be represented by electrostatic and bio-affinity interactions. Probably, the first contact was mainly electrostatic while the His-Ni(II) coordination developed later due to orientation constrains. At low degree of surface coverage, His_6-H49 molecules had time and room to achieve the proper orientation for the bio-affinity interaction ($\tau_{75} \sim \tau_{op}$) whereas the orientation restriction was more evident at high degree of surface coverage.

His_6-H49 desorption behavior at high degree of surface coverage was further evaluated with different compounds. Non-specific washing with surfactant (anionic, cationic or neutral) solutions did not remove either physical adsorbed nor surface coordinated antigens. CTAB and SDS were adsorbed on the free surface sites failing to remove the protein layer. Tween 20, a surfactant usually employed in preventing the physical adsorption of antibodies present in serum during the immunoreaction, did not adsorb on the free surface sites nor induced desorption of adsorbed protein. Specific desorption agents (His and Imi) that directly competed with the His-tag antigen for the surface Ni(II) sites [40] were also used. Fig. 6 compares the desorbed percentages after rinsing with each agent in the presence and absence of Ni(II). NaCl was also included to account for the effect of the ionic strength and PB for comparison

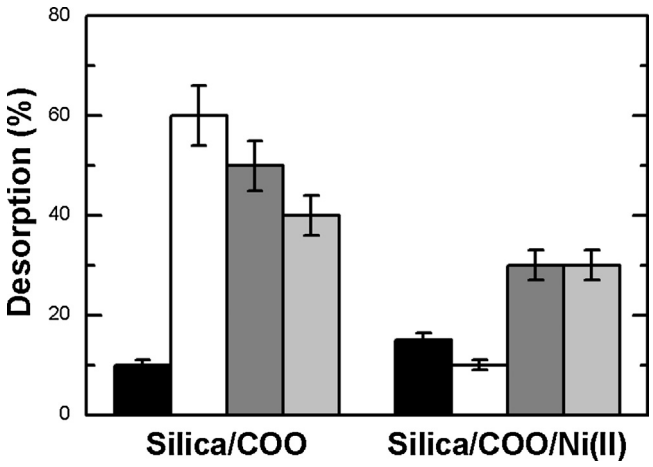

Fig. 6. Desorption percentages of His_6-H49 from silica/COO and silica/COO-Ni(II) upon rinsing with PB (black), 0.2 mol L^{-1} NaCl (white), 0.2 mol L^{-1} His (dark gray), and 0.5 mol L^{-1} Imi (light gray) solutions. The percentage values and the error bars were calculated from the mean and standard deviation of three independent measurements, respectively.

purposes. His and Imi had the same effect as NaCl solutions when desorbing His_6-H49 from silica/COO, removing around 50% of the adsorbed antigen molecules. On the other hand, NaCl only removed 10% while the specific competitors up to 30% when His_6-H49 was adsorbed on the Ni(II) modified substrate.

In summary, physically adsorption of His_6-H49 was present on the modified substrate either in the absence or in the presence of Ni(II). When bio-affinity interactions were feasible, the adsorption process took place in two competitive stages which were related to a first electrostatic interaction followed by the surface complex formation between the His residues and Ni(II) sites. This two-stages process was related to orientation constrains imposed by the size of the tag compared to the whole antigen and caused a stable surface bio-functionalization (strong antigen–substrate interaction without structural changes). Most of the physically adsorbed antigens were removed by simply washing with NaCl solutions at high degree of surface coverage, which represented a simple and easy strategy to prepare bio-functional surfaces. Further, these bio-functional surfaces may be re-used after exhausting washing with Imi and/or His solutions.

4.3. His_6-H49 surface bio-activity

To evaluate the biological activity, the bio-functional surface was prepared on gold/COO-Ni(II) substrate using the optimized conditions (adsorption in PB and high degree of surface coverage and rinsing with PB, followed by NaCl). Modified gold substrates can be coupled to electrochemical methods [26] to directly detect the bio-recognition event, as usually performed with redox enzymes [41]. Particularly, the electrochemical response of the $K_3Fe(CN)_6/K_4Fe(CN)_6$ redox probe was followed by CV to evaluate the surface immunoreaction. The idea behind these experiments was that the redox reaction of the probe would appear less reversible, due to the lower electron transfer rate at the electrode, after the interaction of the bio-functional surface with positive Chagas serum. Experimentally, this reversibility change is reflected in the peak separation between the oxidation and reduction waves (ΔE_p) of the CV, particularly at high scan rates [42]. An electrochemically reversible one-electron process produces $\Delta E_p = 60$ mV while decreasing the electron-transfer kinetics through the working electrode increases ΔE_p [42].

Fig. 7A shows the CV of the redox probe using the bio-functional surface as the working electrode before and after the

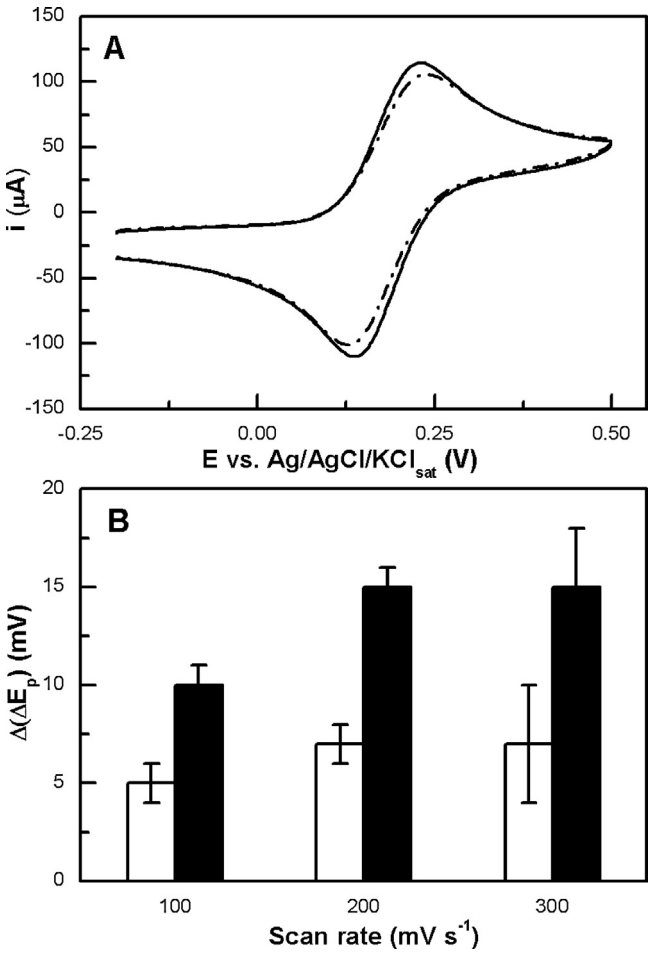

Fig. 7. (A) CV of the redox probe $K_4Fe(CN)_6/K_3Fe(CN)_6$ on the bio-functional surface before (solid line) and after (dot-dashed line) the immunoreactions at 300 mV s^{-1}. (B) $\Delta(\Delta E_p)$ for the redox probe on the bio-functional surface after treatment with negative (white) and positive (black) Chagas sera. The values and the error bars were calculated from the mean and standard deviation of three independent measurements, respectively.

immunoreaction at 300 mV s^{-1}. The measured CV prior to the immune reaction revealed well defined waves corresponding to the $[Fe(CN)_6]^{4-}/[Fe(CN)_6]^{3-}$ redox reaction with $\Delta E_p = 90$ mV. This peak separation larger than 60 mV indicated that the electron-transfer rate through the bio-functional surface was slower than trough bare gold [26]. After the immunoreaction, $\Delta E_p = 106$ mV indicating a further diminution of the electron transfer kinetics through the working electrode when the immune complex was on the bio-functional surface. Based on these results, the analytical response to evaluate the surface bio-activity was defined as:

$$\Delta(\Delta E_p) = \Delta E_{p(\mathrm{IR})} - \Delta E_{p(\mathrm{BS})}$$

where $\Delta E_{p(\mathrm{BS})}$ and $\Delta E_{p(\mathrm{IR})}$ represent ΔE_p values before and after the immunoreaction, respectively. Fig. 7B shows $\Delta(\Delta E_p)$ values before and after dipping the bio-functional surface in positive (black bars) and negative (white bars) sera as a function of the scan rate. The non-zero $\Delta(\Delta E_p)$ values of negative sera were assigned to the interference of the enormous amount of different compounds present in the analyte sample. It is important to point out that the bio-activity experiments could not be optimized by using a purified antibody as usually performed with other immunosensors or biosensors [23]. Dipping in serum was the only way to check the surface bio-functionality. Nevertheless, at scan rates higher than 100 mV s^{-1}

the presence of Chagas antibodies in the sample produced $\Delta(\Delta E_p)$ values significantly different ($p < 0.05$) than those measured with negative sera. First, these surface bio-activity experiments indicated that His_6-H49 on Ni(II) modified substrates adopted the proper orientation and kept the native conformation necessary to specifically recognize Chagas antibodies. Further, these results clearly highlighted that a rather simple and direct electrochemical technique could be coupled to the bio-functional surface to detect Chagas antibodies. Finally, the bio-functional surface may also be coupled to electrochemical impedance spectroscopy [43–45] to determine the electron-transfer constants before and after the immunoreaction, as a more advanced analytical response.

5. Conclusions

His_6-H49 adsorbs on Ni(II) modified substrates through electrostatic and bio-affinity interactions. Physical adsorption results in randomly oriented antigens while bio-affinity interactions in site oriented molecules on the substrate. The bio-affinity interaction causes a strong coordination bond between the histidine residues of the antigen and the Ni(II) surface sites which can only be removed with high concentrations of specific competitors. On the other hand, physical adsorption is minimized by using conditions of electrostatic repulsion (pH and ionic strength), high degree of surface coverage and further removal by washing with unspecific agents. Under these conditions all the capabilities of the strong surface chelate are exploited to develop bio-functional surfaces with appropriate bio-recognition response that can be detected with direct, non-labeled electrochemical methods.

The collected results demonstrate a rational development of bio-functional surfaces to design innovative tools for immunosensors, which can be potentially used in immune-based diagnosis of different illness and infections, such as the neglected Chagas disease.

Acknowledgments

The authors acknowledge FonCyT, SeCyT-UNC and CONICET for financial support. LEV thanks CONICET for fellowships. The authors gratefully acknowledge S. Gea, E. Moretti and J. F. Da Silveira for the Chagas samples and the plasmid vector, respectively.

References

[1] C. Ponce, E. Ponce, E. Vinelli, A. Montoya, V.D. Aguilar, A. Gonzalez, B. Zingales, R. Rangel-aldao, M.J. Levin, J. Esfandiari, E.S. Umezawa, A.O. Luquetti, J. Clin. Microbiol. 43 (2005) 5065.
[2] WHO, Consultation on International Biological Reference Preparations for Chagas Diagnostic Tests Organization, World Health Organization, 2007.
[3] Z.C. Caballero, O.E. Sousa, W.P. Marques, A. Saez-Alquezar, E.S. Umezawa, Clin. Vacc. Immunol. 14 (2007) 1045.
[4] A.M. Afonso, M.H. Ebell, R.L. Tarleton, PLoS Neglec. Trop. Dis. 6 (2012).
[5] A.A.P. Ferreira, W. Colli, P.I. da Costa, H. Yamanaka, Biosens. Bioelectron 21 (2005) 175.
[6] E. Salinas, A.A.J. Torriero, F. Battaglini, M.I. Sanz, R. Olsina, J. Raba, Biosens. Bioelectron 21 (2005) 313.
[7] M.E. Ribone, M.S. Belluzo, D. Pagani, I.S. Macipar, C.M. Lagier, Anal. Biochem. 350 (2006) 61.
[8] S.V. Pereira, F.A. Bertolino, M.A. Fernandez-Baldo, G.A. Messina, E. Salinas, M.I. Sanz, J. Raba, Analyst 136 (2011) 4745.
[9] M.S. Belluzo, M.É. Ribone, C. Camussone, I.S. Marcipar, C.M. Lagier, Anal. Biochem. 408 (2011) 86.
[10] C. Camussone, V. Gonzalez, M.S. Belluzo, N. Pujato, M.E. Ribone, C.M. Lagier, I.S. Marcipar, Clin. Vacc. Immunol. 16 (2009) 899.
[11] J.F. da Silveira, E.S. Umezawa, a.O. Luquetti, Trends Parasitol. 17 (2001) 286.
[12] P.C. Cotrim, G.S. Paranhos, R.A. Mortara, J. Wanderley, A. Rassi, M.E. Camargo, J. Franco Da Silveira, J. Clin. Microbiol. 28 (1990) 519.
[13] E.S. Umezawa, S.F. Bastos, M.E. Camargo, L.M. Yamauchi, M.R. Santos, A. Gonzalez, B. Zingales, M.J. Levin, O. Sousa, R. Rangel-Aldao, J. Franco Da Silveira, J. Clin. Microbiol. 37 (1999) 1554.
[14] B. Kasemo, Surf. Sci. 500 (2002) 656.
[15] C.L. Smith, S.M. Giang, Top. Curr. Chem. 261 (2006) 63.
[16] P.a. Millner, H.C.W. Hays, a. Vakurov, N.a. Pchelintsev, M.M. Billah, M.a. Rodgers, Semin. Cell Dev. Biol. 20 (2009) 34.
[17] L.E. Valenti, C.P. De Pauli, C.E. Giacomelli, J. Inorg. Biochem. 100 (2006) 192.
[18] L. Nieba, S.E. Nieba-Axmann, a. Persson, M. Hämäläinen, F. Edebratt, a. Hansson, J. Lidholm, K. Magnusson, a.F. Karlsson, a. Plückthun, Anal. Biochem. 252 (1997) 217.
[19] C. Jones, A. Patel, S. Griffin, J. Martin, P. Young, K. O'Donnell, C. Silverman, T. Porter, I. Chaiken, J. Chromatogr. A 707 (1995) 3.
[20] X.-M. Li, X.-Y. Yang, S.-S. Zhang, TrAC Trends Anal. Chem. 27 (2008) 543.
[21] N. Kim, D.K. Kim, Y.J. Cho, Curr. App. Phys. 10 (2010) 1227.
[22] S.J. Kim, K.V. Gobi, R. Harada, D.R. Shankaran, N. Miura, Sens. Actuators B 115 (2006) 349.
[23] R.E. Ionescu, S. Cosnier, S. Herrmann, R.S. Marks, Anal. Chem. 79 (2007) 8662.
[24] J. Huang, Q. Lin, X. Zhang, X. He, X. Xing, W. Lian, M. Zuo, Q. Zhang, Food Res. Int. 44 (2011) 92.
[25] C.E. Giacomelli, L.E. Valenti, M.L. Carot, Biomolecules and solid substrate interaction: key factors in developing biofunctional surfaces, in: Encyclopedia of Surface and Colloid Science, second ed., Taylor & Francis, Oxford, U.K., 2012, pp. 1.
[26] L.E. Valenti, V.L. Martin, E. Herrera, R.M. Torresi, C.E. Giacomelli, J. Mater. Chem. B (2013), http://dx.doi.org/10.1039/c3tb20769b (in press).
[27] L.E. Valenti, P.A. Fiorito, C.D. García, C.E. Giacomelli, J. Colloid Interface Sci. 307 (2007) 349.
[28] E.L. Schmid, T.A. Keller, Z. Dienes, H. Vogel, Anal. Chem. 69 (1997) 1979.
[29] C. Geffroy, M.P. Labeau, K. Wong, B. Cabane, M.A. Cohen Stuart, Colloids Surf., A 172 (2000) 47.
[30] J.C. Dijt, M.A.C. Stuart, G.J. Fleer, Adv. Colloid Interface Sci. 50 (1994) 79.
[31] J.C. Dijt, M.A.C. Stuart, J.E. Hofman, G.J. Fleer, Colloids Surf. 51 (1990) 141.
[32] R. Atkin, V.S.J. Craig, E.J. Wanless, S. Biggs, J. Colloid Interface Sci. 266 (2003) 236.
[33] E. Gasteiger, Hoogland, C., Gattiker, A., Duvaud, S.e., Wilkins, M., Appel, R., Bairoch, A., Protein identification and analysis tools on the expasy server, in: J. Walker (Ed.), The Proteomics Protocols Handbook, Humana Press, NJ, USA, 2005, p. 571.
[34] Valenti, L.E., Desde La Optimización De La Interacción Proteína-Superficie Hacia La Obtención De Inmunoensayos En Fase Sólida. Ph.D. Thesis. Facultad de Ciencias Quimicas. Universidad Nacional de Córdoba, Córdoba, Argentina, 2008.
[35] C.F. Wertz, M.M. Santore, Langmuir 17 (2001) 3006.
[36] M. van der Veen, M.C. Stuart, W. Norde, Colloids Surf. B 54 (2007) 136.
[37] M.M. Santore, C.F. Wertz, Langmuir 21 (2005) 10172.
[38] W. Norde, C.E. Giacomelli, J. Biotechnol. 79 (2000) 259.
[39] C.E. Giacomelli, W. Norde, J. Colloid Interface Sci. 233 (2001) 234.
[40] E. Kang, J.-W. Park, S.J. McClellan, J.-M. Kim, D.P. Holland, G.U. Lee, E.I. Franses, K. Park, D.H. Thompson, Langmuir 23 (2007) 6281.
[41] K. Haberska, O. Svensson, S. Shleev, L. Lindh, T. Arnebrant, T. Ruzgas, Talanta 76 (2008) 1159.
[42] R.S. Nicholson, Anal. Chem. 37 (1965) 1351.
[43] S. Grimnes, Ø.G. Martinsen, Bioimpedance and Bioelectricity Basics, second ed., Elsevier Ltd., Oxford, UK, 2008.
[44] M.E. Orazem, B. Tribollet, Electrochemical Impedance Spectroscopy, John Willey & Sons, Inc., NJ, USA, 2008.
[45] E. Barsoukov, J.R. Macdonald (Eds.), Impedance Spectroscopy Theory, Experiment, and Applications, second ed., John Willey & Sons, Inc., NJ, USA, 2005.